Supporting Information

Vertical Kinetically Oriented MoS_2-Mo_2N Heterostructure on Carbon Cloth: A Highly Efficient Hydrogen Evolution Electrocatalyst

Chao Huang,[1] Qingdong Ruan,[1] Hao Song,[1,2] Yang Luo,[1] Hongzhen Bai,[1] Biao Gao,[1,2] and Paul K. Chu[1*]

[1] Department of Physics, Department of Materials Science and Engineering, and Department of Biomedical Engineering, City University of Hong Kong, Tat Chee Avenue, Kowloon, Hong Kong, China

[2] The State Key Laboratory of Refractories and Metallurgy and Institute of Advanced Materials and Nanotechnology, Wuhan University of Science and Technology, Wuhan 430081, P. R. China

[*]Corresponding author:

E-mail: paul.chu@cityu.edu.hk (P.K. Chu)

Electrochemical Active Surface Area

The electrochemical active surface area (ECSA) of the catalysts was determined using the electrochemical double-layer capacitance (C_{dl}). To measure C_{dl}, the CV curves were collected in the nonfaradic region from 0.15 to 0.25 V using scanning rates between 10 mV s^{-1} and 100 mV s^{-1}. The ECSA value (A_{ECSA}) was converted by using C_{dl} versus a flat standard with a real surface area of 1 cm^2 as follows:

$$A_{ECSA} = \frac{\text{electrochemical capacitance}}{40\ \mu F\ cm^{-2}\ \text{per}\ cm^2_{ECSA}}, \quad (1)$$

where Cs is the specific capacitance of the sample per area under the same electrolyte conditions. According to the previous report, a value of 40 uF cm^{-2} is suitable for the experiment.[1, 2]

Turnover Frequency Calculation

The turnover frequency was calculated by the following formula:

$$TOF = \frac{\text{no. of total hydrogen turnovers/ } cm^2 \text{ of geometric area}}{\text{no. of active sites/ } cm^2 \text{ of geometric area}}.$$

The total number of hydrogen turnover per current density was calculated by the formula:

$$\text{No. of } H_2 = (\text{per } \frac{mA}{cm^2})(\frac{1\ C\ s^{-1}}{1000\ mA})(\frac{1\ \text{mol of e}}{96485.3\ C})(\frac{1\ \text{mol of } H_2}{2\ \text{mol of e}})(\frac{6.022 \times 10^{23} H_2\ \text{molecules}}{1\ \text{mol of } H_2})$$

$$= 3.12\times10^{15}\ \frac{H_2\ s^{-1}}{cm^2}\ \text{per}\ \frac{mA}{cm^2}$$

Active sites per real surface area

Mo atoms were assumed to be the active sites on MoS_2 and did not change during HER:

$$\text{Active sites} = (\frac{2\ \text{atoms/ unit cell}}{37.2\ Å^3/\ \text{unit cell}})^{\frac{2}{3}} = 1.42\times10^{15}\ \text{atoms cm-2 real.}$$

The current density plot was converted into a TOF plot according to the following:

$$\text{TOF} = \frac{(3.12 \times 1015\ \frac{H_2\ s^{-1}}{cm^2}\ \text{per}\ \frac{mA}{cm^2}) \times |j|}{(\text{active sites per real surface area}) \times A_{ECSA}}.$$

Theoretical calculation

The first-principles density functional theory (DFT) calculation was performed based on the Cambridge Sequential Total Energy Package known as CASTEP.[3] The exchange-correlation functional under the generalized gradient approximation (GGA)[4]

with norm-conserving pseudopotentials and Perdew-Burke-Ernzerhof (PBE) functional was adopted to describe the electron-electron interactions.[5] To optimize the geometry, all the atoms were allowed to relax completely until the force exerted on each atom was less than 0.01 eV/Å. The K-point set of 5 × 5 × 1 was tested to be convergent and the energy cutoff was 550 eV. To construct the heterojunction of MoS_2-Mo_2N, the cleavage surface of (002) of MoS_2 and (111) of Mo_2N was constructed. To fully relax the local lattice for adsorption, a 20 Å vacuum space was introduced along the z direction.

The free energy change ΔG of the reaction was calculated as the difference between the free energies of the initial and final states as shown in the following:

$$\Delta E = E_{*H} - (E_{*} + E_{H}) \text{ and} \quad (1)$$

$$\Delta G = \Delta E + \Delta ZPE - T\Delta S, \quad (2)$$

where ΔE is the adsorption energy of H atom on the surface, ΔZPE is the zero-point energy, ΔS denotes the entropy change of *H, (ΔZPE - $T\Delta S$) is 0.24 eV[6, 7], and $\Delta G = \Delta E$ + 0.24eV.[8]

Systems	ΔG
Mo_2N-Mo	-3.59
Mo_2N-N	-3.89
MoS_2-edge	0.39
MoS_2-basal	1.95
MoS_2-Mo_2N	-0.079

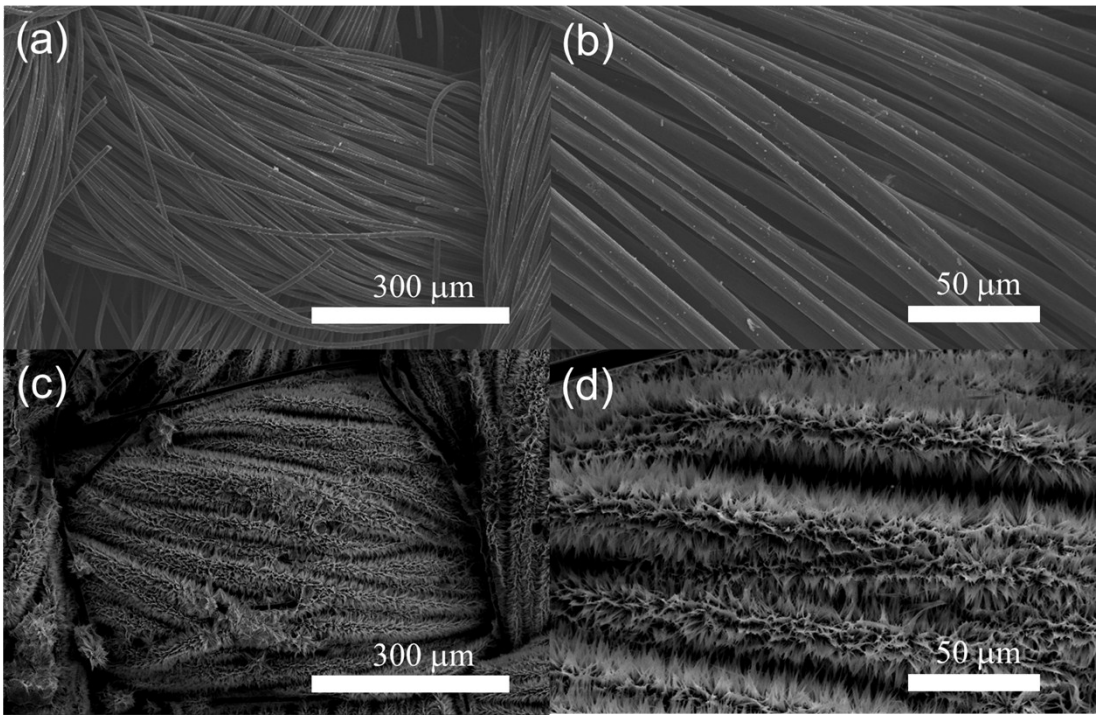

Figure S1. Morphology of (a and b) Pristine carbon cloth (CC) and (c and d) MoO_3 nanoneedles grown on CC.

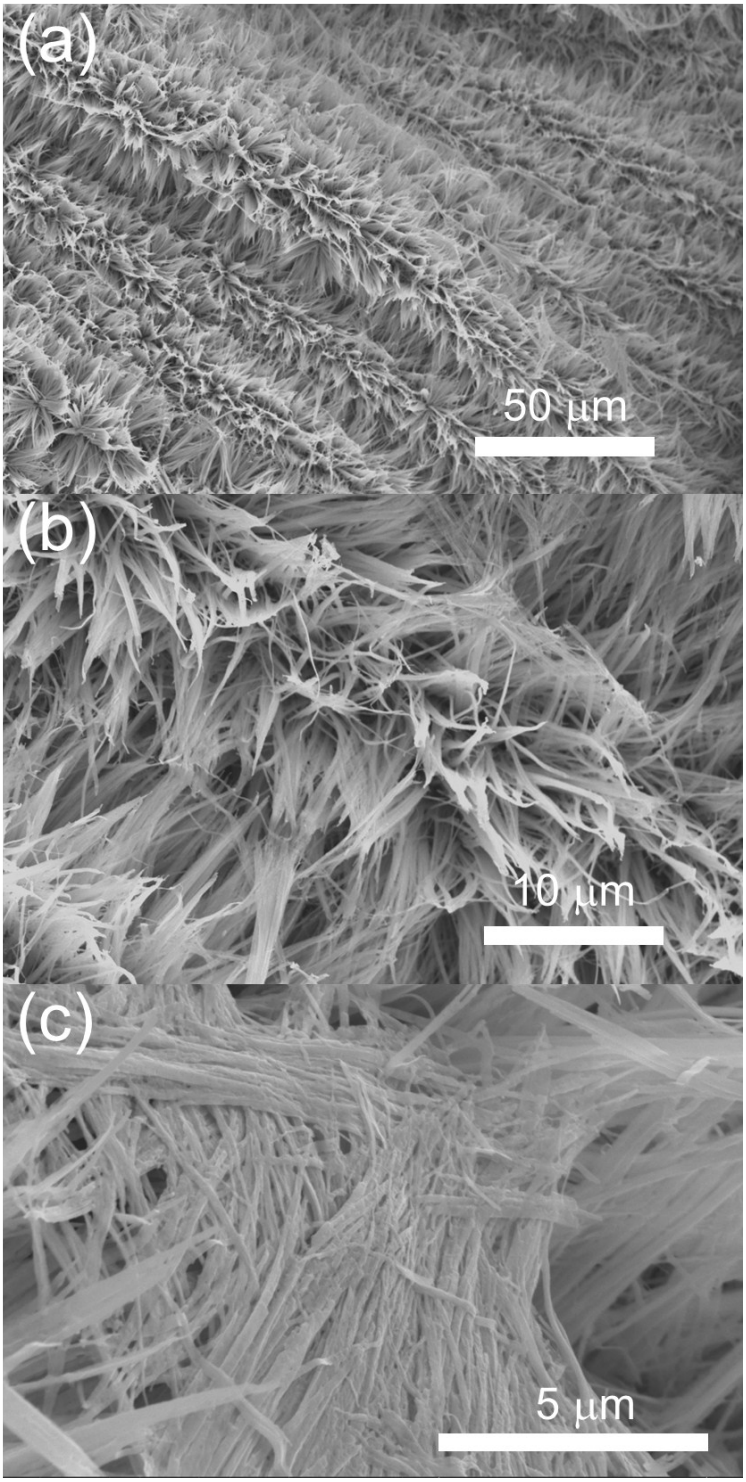

Figure S2. SEM images of Mo_2N/CC.

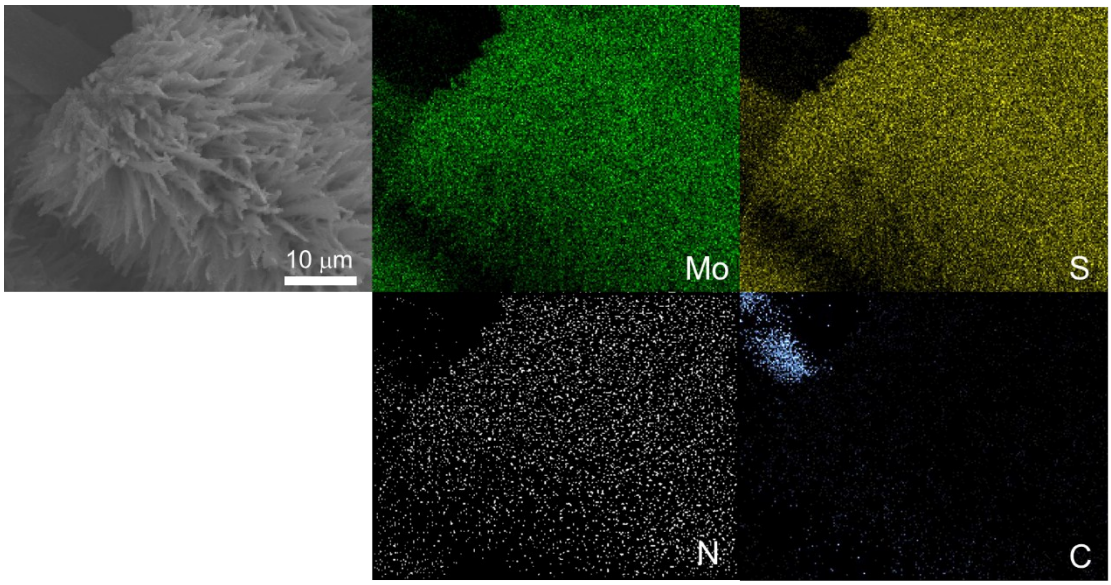

Figure S3. Elemental maps of MoS_2-Mo_2N/CC.

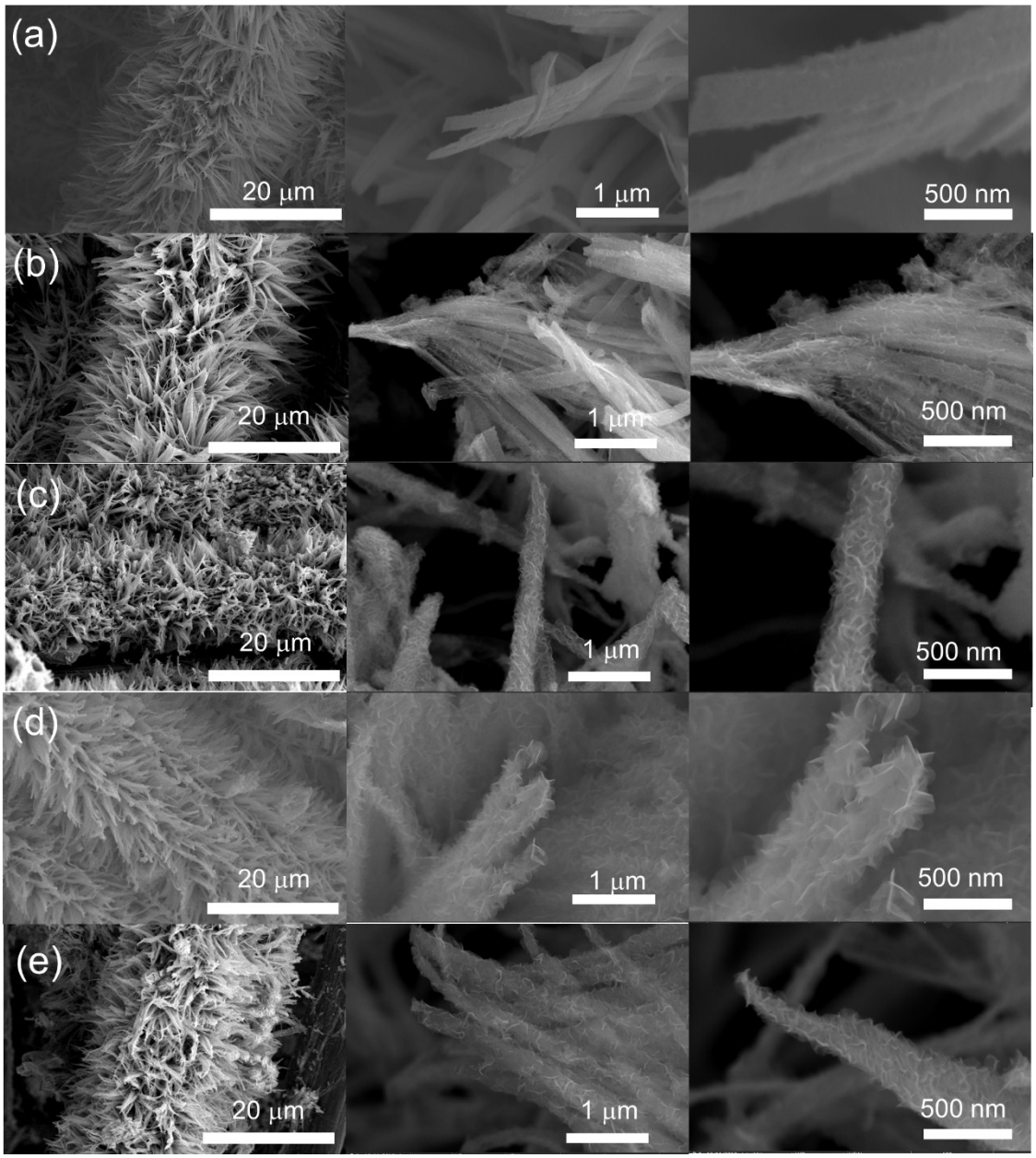

Figure S4. Morphology of Mo_2N/CC transferred to a Teflon-line stainless steel autoclave with $CS(NH_2)_2$ and H_2O and heating to 220 ^oC for: (a) 4 h, (b) 8 h, (c)16 h, (d) 24 h, and (e) 32 h.

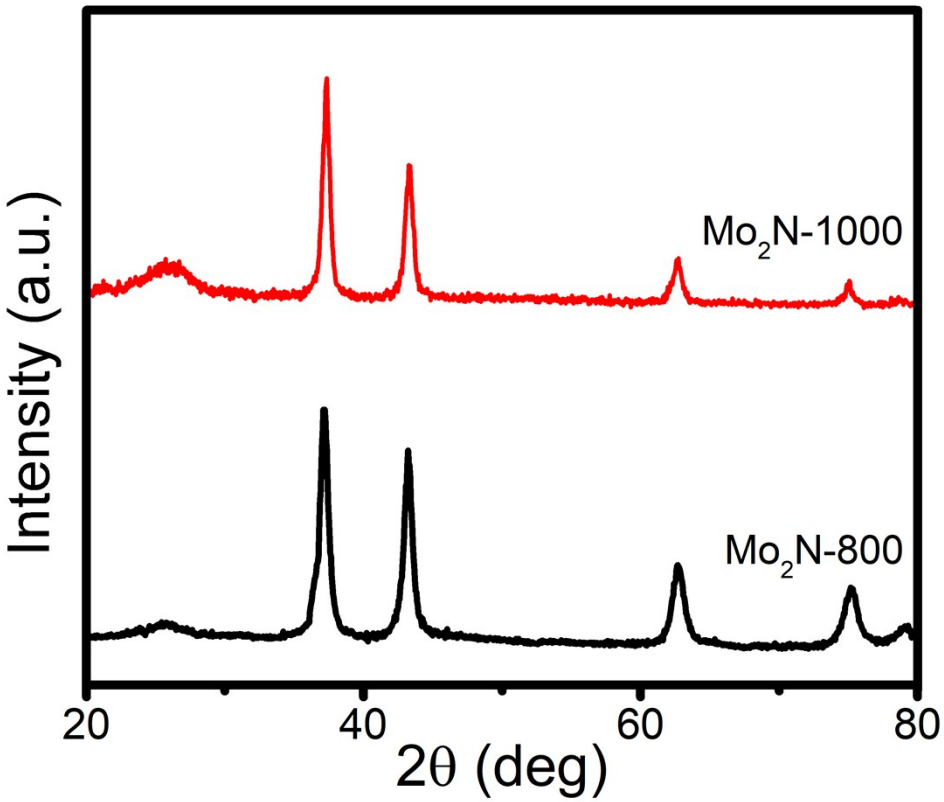

Figure S5. XRD spectra of MoO_3/CC annealed at 1000 ^oC and 800 ^oC in NH_3.

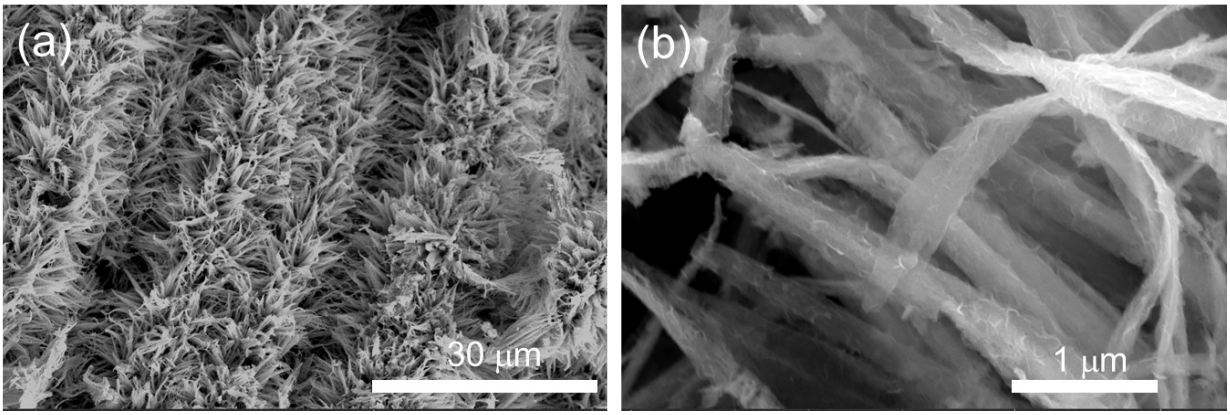

Figure S6. Morphology of Mo_2N/CC annealed at 1000 ^oC and then treated hydrothermally for 24 h.

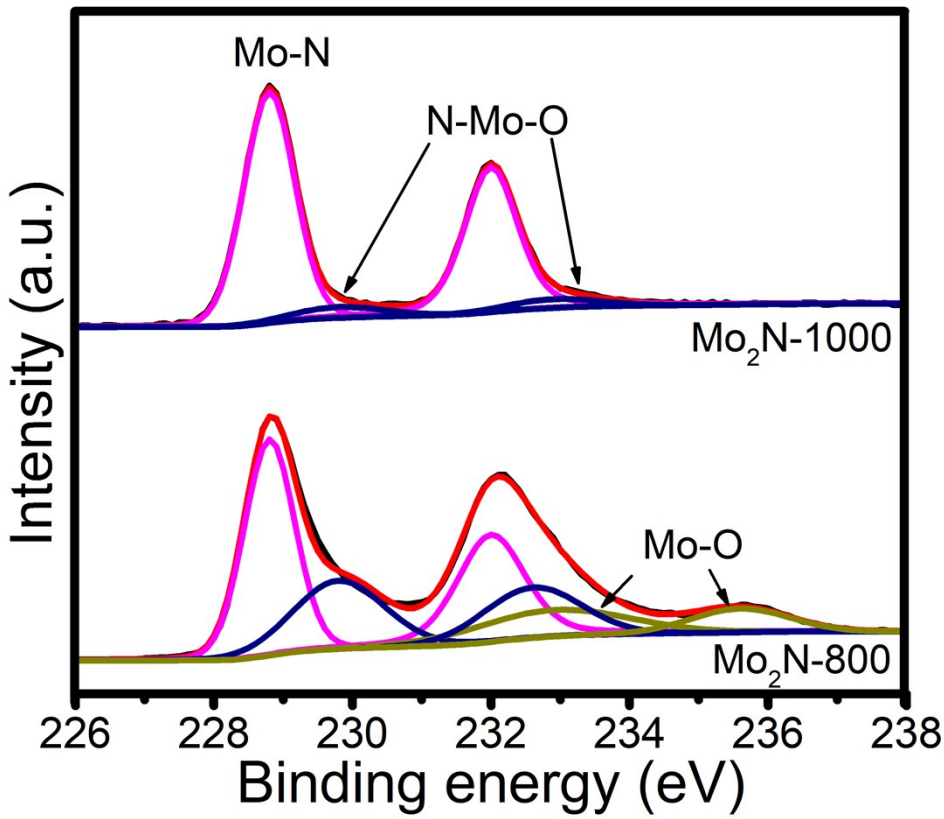

Figure S7. XPS spectra of MoO_3/CC annealed at 1000 ^oC and 800 ^oC in NH_3.

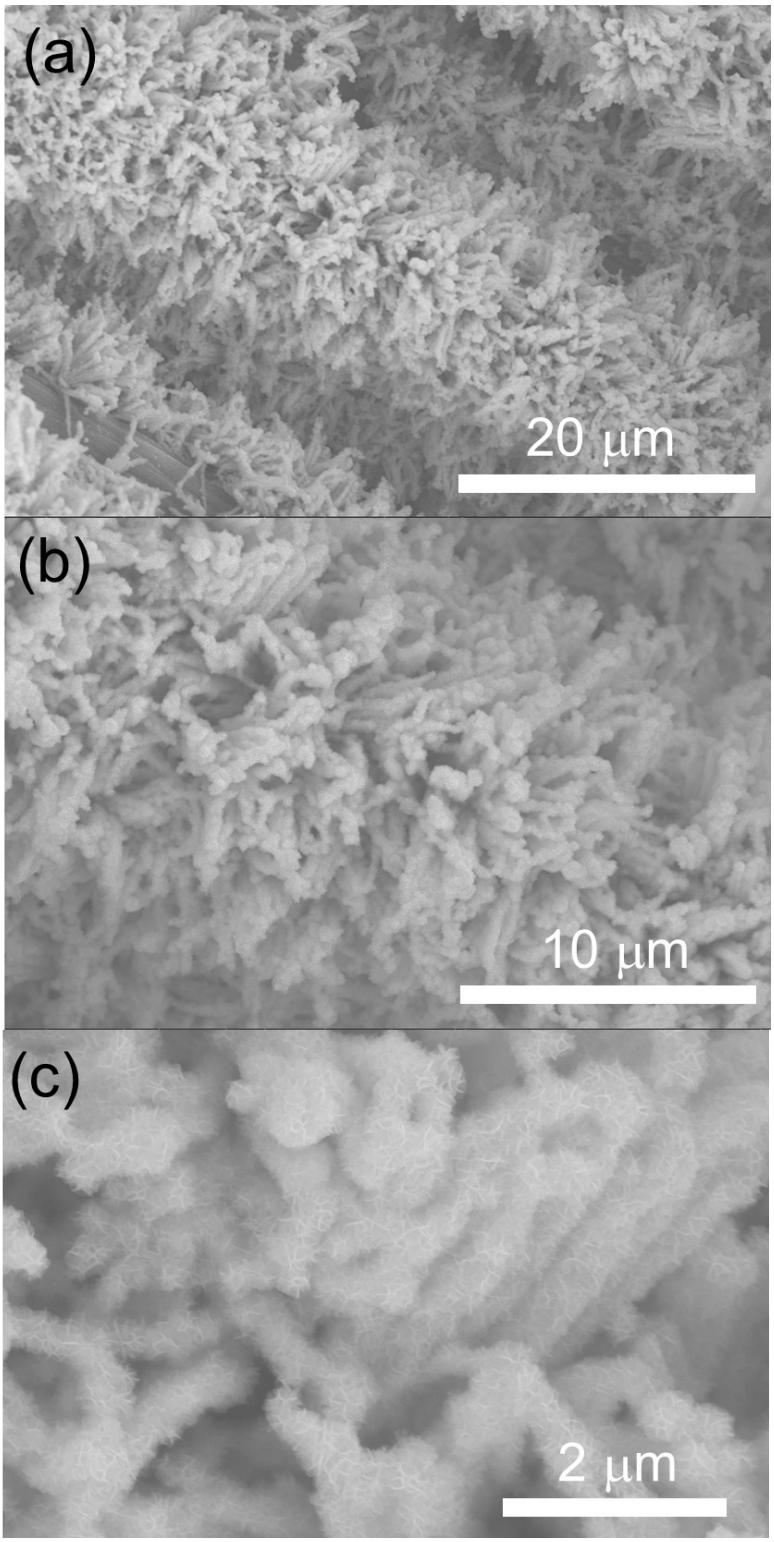

Figure S8. SEM images of MoS_2/CC.

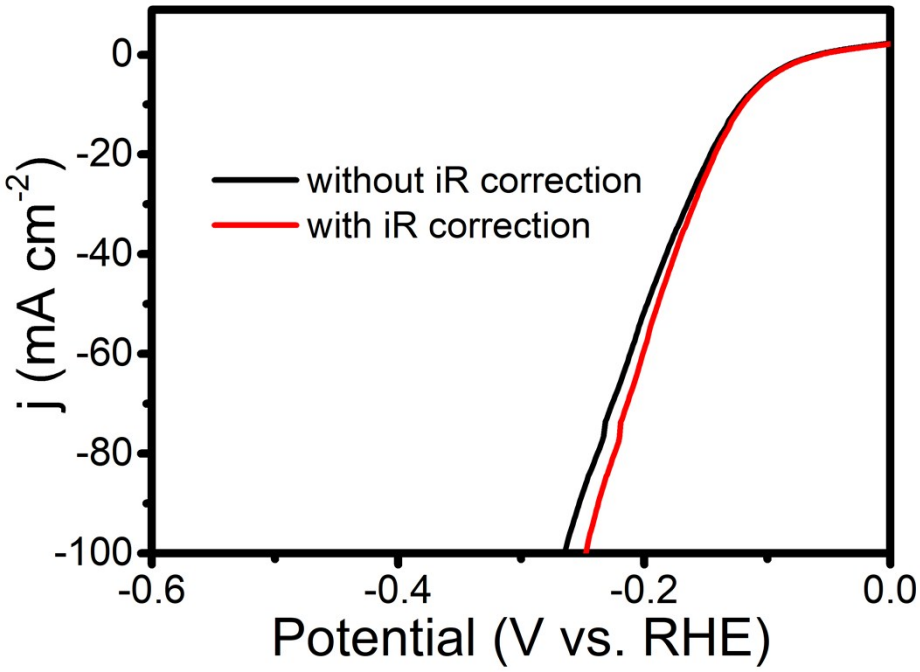

Figure S9. Polarization curves of MoS_2-Mo_2N/CC with and without iR correction.

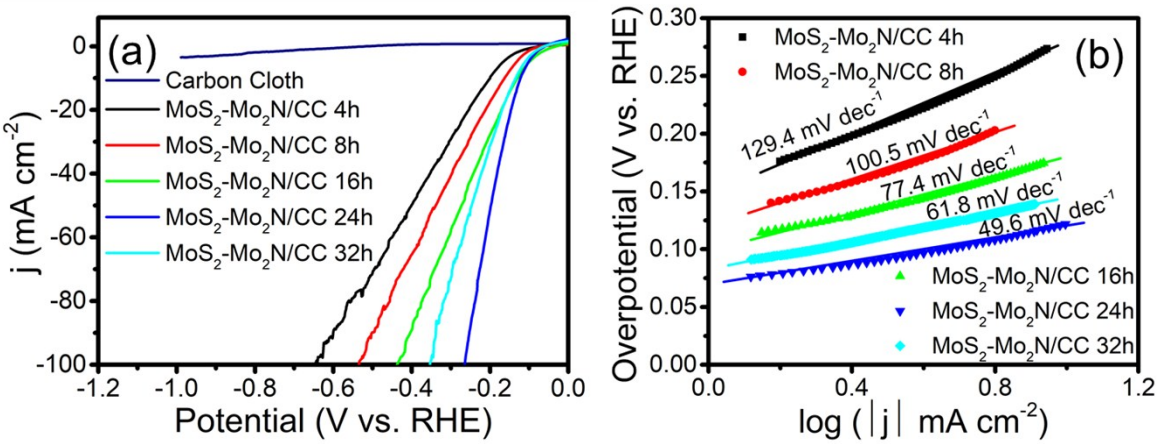

Figure S10. (a) Polarization curves of MoS_2-Mo_2N/CC annealed for difference time and (b) Corresponding Tafel slopes.

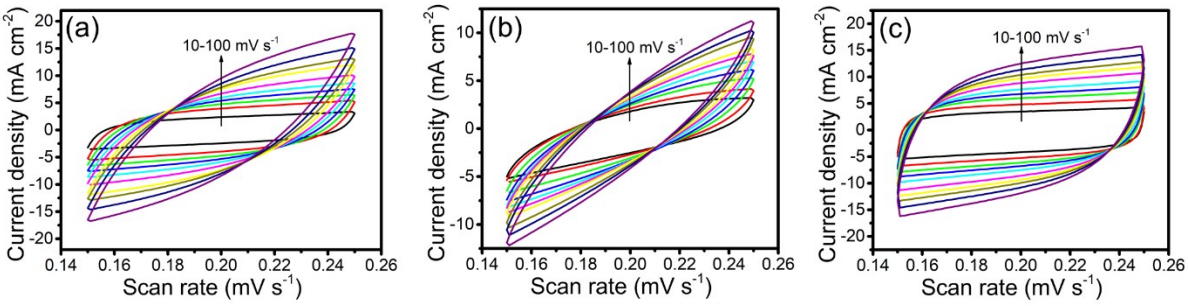

Figure S11. CV curves of (a) MoS_2-Mo_2N/CC, (b) MoS_2/CC, and (c) Mo_2N/CC.

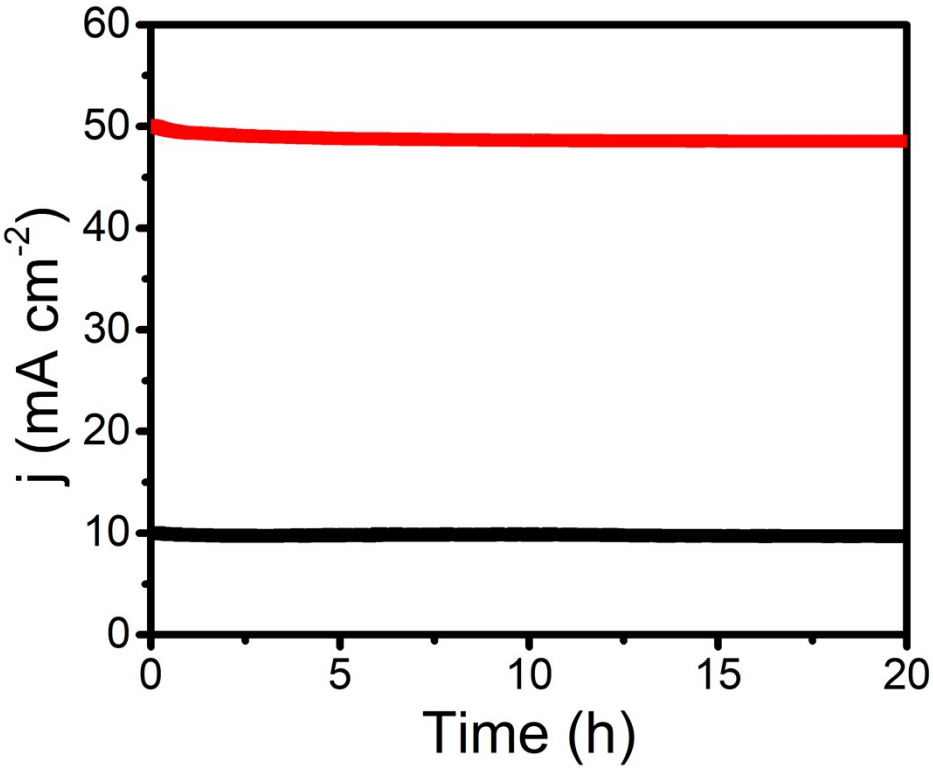

Figure S12. HER stability of MoS_2-Mo_2N/CC at 10 mA cm^{-2} and 50 mA cm^{-2}.

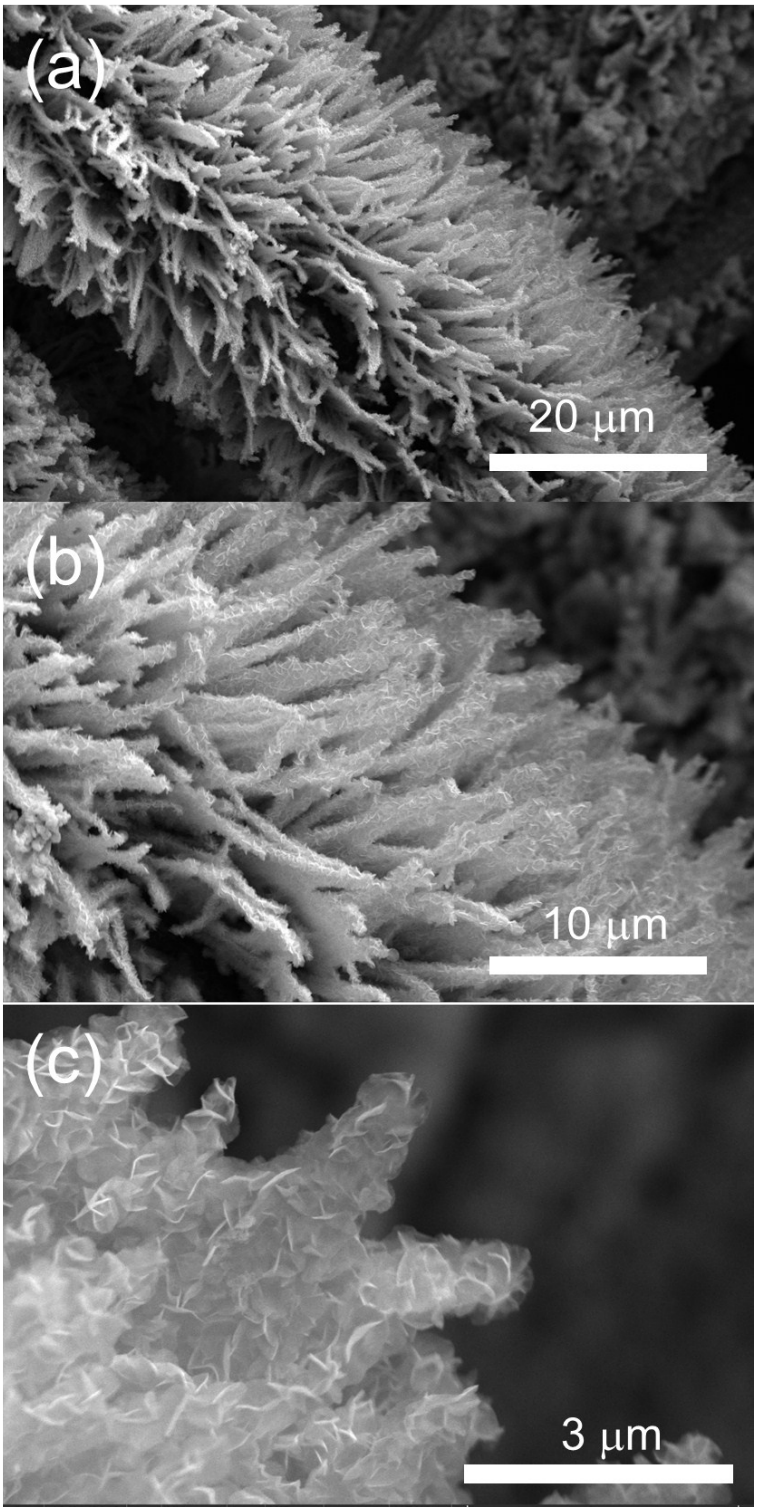

Figure S13. SEM images of MoS_2-Mo_2N/CC after long-term HER stability assessment.

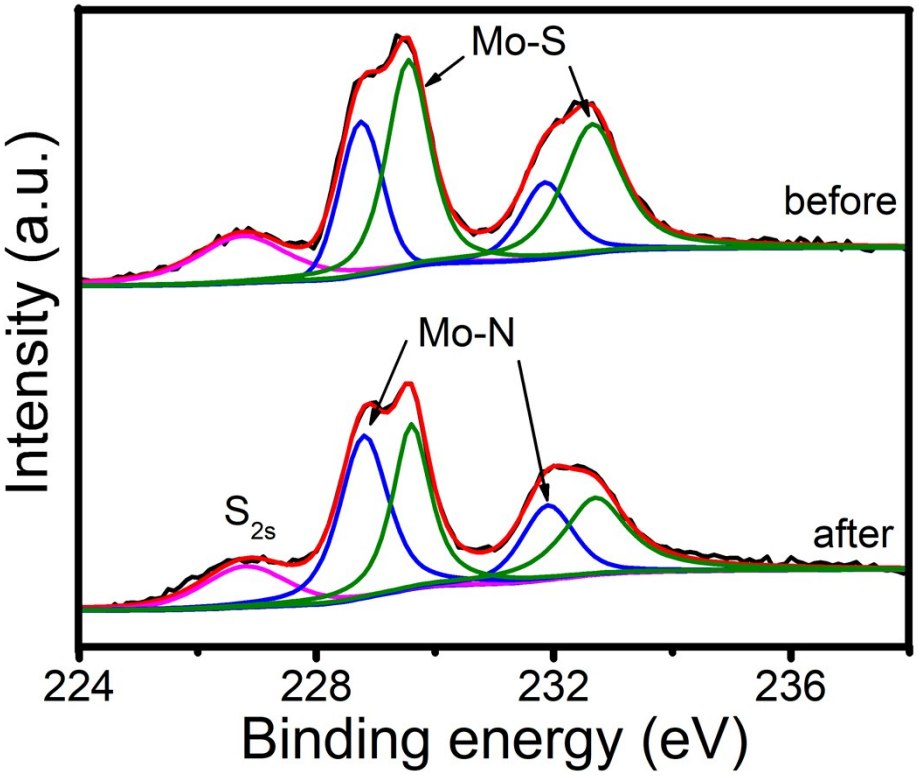

Figure S14. XPS spectra of MoS_2-Mo_2N/CC before and after the i-t test.

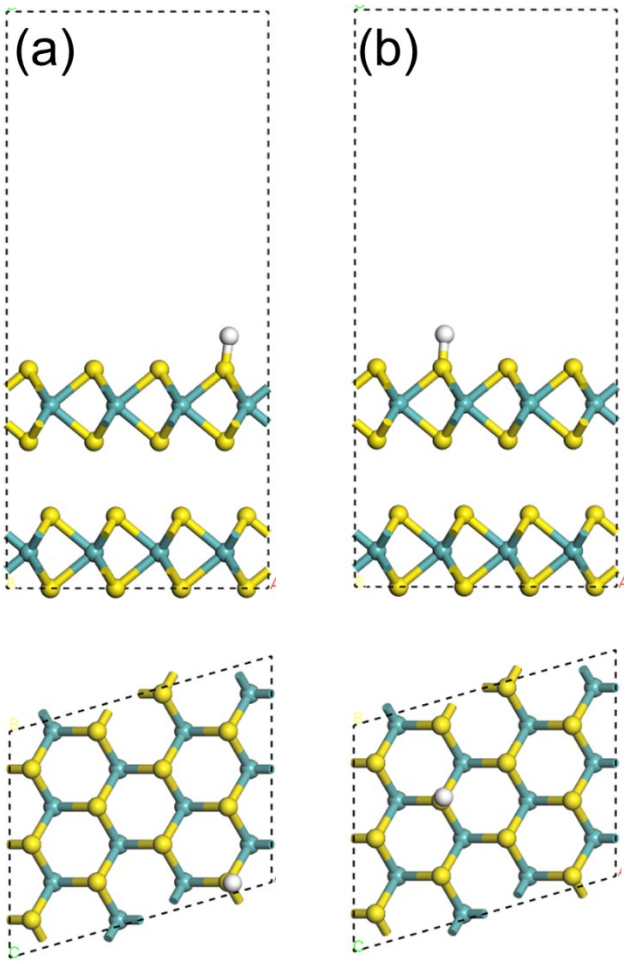

Figure S15. Adsorption of H atoms on (a) Edge and (b) Basal plate of MoS_2.

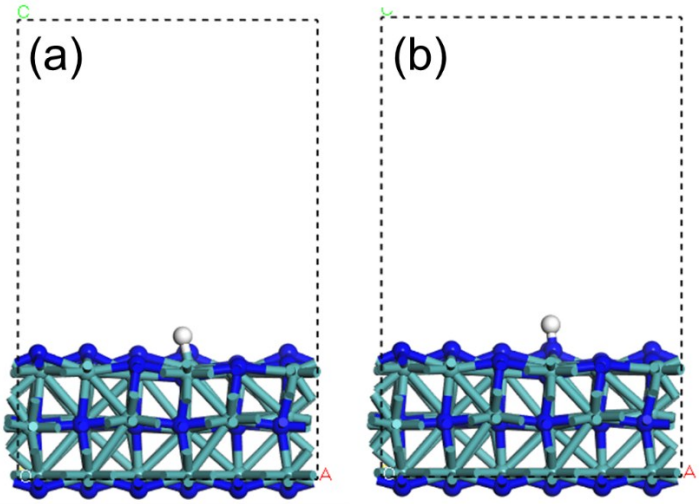

Figure S16. Adsorption of H atoms on (a) Mo site and (b) N site.

Table S1. Comparison of the properties MoS_2-based catalysts for HER.

Electrodes	media	Overpotential (mV) (10 mA cm^{-2})	Overpotential (mV) (100 mA cm^{-2})	Tafel slope (mV dec^{-1})	References
MoS_2-Mo_2N/CC	0.5M H_2SO_4	121	264	49.6	This work
MoS_2@NSCS	0.5M H_2SO_4	158	320 (~60 mA cm^{-2})	82	[9]
Vertically aligned MoS_2	0.5M H_2SO_4	250	~600 (~60 mA cm^{-2})	74	[10]
$MoS_{2(1-x)}Se_2$	0.5M H_2SO_4	164	480 (~55 mA cm^{-2})	48	[11]
hH-MoS_2	0.5M H_2SO_4	214	~300 (~60 mA cm^{-2})	74	[12]
$MoWS_2$/CC	0.5M H_2SO_4	145	~200 (~40 mA cm^{-2})	46.7	[13]
CoP/CN@MoS_2	0.5M H_2SO_4	144	220 (~80 mA cm^{-2})	69	[14]
Au-MoS_2	0.5M H_2SO_4	170	250 (~32 mA cm^{-2})	60	[15]
Zn-MoS_2	0.5M H_2SO_4	130	250	51	[16]
MoS2 QDs/rGO	0.5M H_2SO_4	222	300 (~80 mA cm^{-2})	59.8	[17]

MoS_2/C_{800}	0.5M H_2SO_4	207	---	73	[18]
$MoS_{2.7}$@NPG	0.5M H_2SO_4	~220	----	41	[19]

References

1. C. Tang, W. Wang, A. Sun, C. Qi, D. Zhang, Z. Wu and D. Wang, *ACS Catal.*, 2015, **5**, 6956-6963.
2. H. Wang, X. Xiao, S. Liu, C.-L. Chiang, X. Kuai, C.-K. Peng, Y.-C. Lin, X. Meng, J. Zhao and J. Choi, *J. Am. Chem. Soc.*, 2019, **141**, 18578-18584.
3. M. Segall, P. J. Lindan, M. a. Probert, C. J. Pickard, P. J. Hasnip, S. Clark and M. Payne, *J. Phys. Condens. Matter*, 2002, **14**, 2717.
4. J. P. Perdew, K. Burke and M. Ernzerhof, *Phys. Rev. Lett.*, 1996, **77**, 3865.
5. D. Hamann, M. Schlüter and C. Chiang, *Phys. Rev. Lett.*, 1979, **43**, 1494.
6. J. K. Nørskov, T. Bligaard, A. Logadottir, J. Kitchin, J. G. Chen, S. Pandelov and U. Stimming, *J. Electrochem. Soc.*, 2005, **152**, J23-J26.
7. Y. Zhao, C. Chang, F. Teng, Y. Zhao, G. Chen, R. Shi, G. I. Waterhouse, W. Huang and T. Zhang, *Adv. Energy Mater.*, 2017, **7**, 1700005.
8. F. Yang, Y. Zhao, Y. Du, Y. Chen, G. Cheng, S. Chen and W. Luo, *Adv. Energy Mater.*, 2018, 1703489.
9. J.-T. Ren, L. Chen, D.-D. Yang and Z.-Y. Yuan, *Appl. Catal., B* 2019, 118352.
10. A. Bayat, M. Zirak and E. Saievar-Iranizad, *ACS Sustain. Chem. Eng.*, 2018, **6**, 8374-8382.
11. Q. Gong, L. Cheng, C. Liu, M. Zhang, Q. Feng, H. Ye, M. Zeng, L. Xie, Z. Liu and Y. Li, *ACS Catal.*, 2015, **5**, 2213-2219.
12. B. Guo, K. Yu, H. Li, H. Song, Y. Zhang, X. Lei, H. Fu, Y. Tan and Z. Zhu, *ACS Appl. Mater. Interfaces*, 2016, **8**, 5517-5525.

13. D. A. Nguyen, T. S. Le, D. Y. Park, D. Suh and M. S. Jeong, *ACS Appl. Mater. Interfaces*, 2019, **11**, 37550-37558.

14. J.-G. Li, K. Xie, H. Sun, Z. Li, X. Ao, Z. Chen, K. K. Ostrikov, C. Wang and W. Zhang, *ACS Appl. Mater. Interfaces*, 2019, **11**, 36649-36657.

15. H. Li, C. Tsai, A. L. Koh, L. Cai, A. W. Contryman, A. H. Fragapane, J. Zhao, H. S. Han, H. C. Manoharan and F. Abild-Pedersen, *Nat. Mater.* , 2016, **15**, 48.

16. Y. Shi, Y. Zhou, D.-R. Yang, W.-X. Xu, C. Wang, F.-B. Wang, J.-J. Xu, X.-H. Xia and H.-Y. Chen, *J. Am. Chem. Soc.*, 2017, **139**, 15479-15485.

17. W. Sun, P. Li, X. Liu, J. Shi, H. Sun, Z. Tao, F. Li and J. Chen, *Nano Research*, 2017, **10**, 2210-2222.

18. H. Sun, X. Ji, Y. Qiu, Y. Zhang, Z. Ma, G.-g. Gao and P. Hu, *J. Alloy. Compd.* 2019, **777**, 514-523.

19. X. Ge, L. Chen, L. Zhang, Y. Wen, A. Hirata and M. Chen, *Adv. Mater.*, 2014, **26**, 3100-3104.